JBC Papers in Press. Published on April 14, 2008 as Manuscript M800907200
The latest version is at http://www.jbc.org/cgi/doi/10.1074/jbc.M800907200

SIGNALING AND CROSSTALK BY C5a AND UDP IN MACROPHAGES SELECTIVELY USE PLCβ3 TO REGULATE INTRACELLULAR FREE CALCIUM.

Tamara I.A. Roach*[1], Robert A. Rebres*[1], Iain D.C. Fraser[3], Dianne L. DeCamp[4], Keng-Mean Lin[4], Paul C. Sternweis[4], Mel I. Simon[3] and William E. Seaman[2].

From the Alliance for Cellular Signaling, [1]Northern California Institute for Research and Education and [2]University of California San Francisco, VA Medical Center, San Francisco, CA 94121, [3]Division of Biology, California Institute of Technology, Pasadena, CA 91125, [4]University of Texas Southwestern Medical Center, Dallas, TX 75390.

* The first two authors made equal contribution to this manuscript.

Running Title: Selective PLCβ3 use in GPCR Ca^{2+} signaling by macrophages

Address correspondence to: Tamara I.A. Roach, Robert A. Rebres or William E. Seaman, VAMC 111R, 4150 Clement Street, San Francisco, CA 94121. Phone:415 750 2104, Fax: 415 750 6920. Email: Tamara.Roach@ucsf.edu, Robert.Rebres@ucsf.edu, bseaman@medicine.ucsf.edu.

Studies in fibroblasts, neurons, and platelets have demonstrated the integration of signals from different G-protein coupled receptors (GPCRs) in raising intracellular free Ca^{2+}. To study signal integration in macrophages, we screened RAW264.7 cells and bone marrow-derived macrophages (BMDM) for their Ca^{2+} response to GPCR ligands. We found a synergistic response to complement component 5a (C5a) in combination with uridine 5'-diphosphate (UDP), platelet activating factor (PAF) or lysophosphatidic acid (LPA). The C5a response was Gαi-dependent, while the UDP, PAF, and LPA responses were Gαq-dependent. Synergy between C5a and UDP, mediated by the C5a and P2Y6 receptors, required dual receptor occupancy, and affected the initial release of Ca^{2+} from intracellular stores as well as sustained Ca^{2+} levels. C5a and UDP synergized in generating inositol-1,4,5-trisphosphate, suggesting synergy in activating phospholipase C (PLC) β. Macrophages expressed transcripts for three PLCβ isoforms (PLCβ2, PLCβ3, and PLCβ4), but GPCR ligands selectively used these isoforms in Ca^{2+} signaling. C5a predominantly used PLCβ3, while UDP used PLCβ3 but also PLCβ4. Neither ligand required PLCβ2. Synergy between C5a and UDP likewise depended primarily on PLCβ3. Importantly, the Ca^{2+} signaling deficiency observed in PLCβ3-deficient BMDM was reversed by re-constitution with PLCβ3. Neither PI-3 kinase nor PKC was required for synergy. In contrast to Ca^{2+}, PI3-kinase activation by C5a was inhibited by UDP, as was macropinocytosis, which depends on PI3-kinase. PLCβ3 may thus provide a selective target for inhibiting Ca^{2+} responses to mediators of inflammation, including C5a, UDP, PAF, and LPA.

Calcium is an important messenger involved in the regulation of multiple cellular processes, and levels of intracellular free calcium ($[Ca^{2+}]_i$) are precisely regulated (1-3). Increases in intracellular $[Ca^{2+}]_i$ are initiated by the phospholipase C (PLC) family of enzymes, which hydrolyze membrane-associated phosphatidylinositol-4,5-diphosphate (PIP_2) to produce inositol-1,4,5-trisphosphate (IP_3) and diacylglycerol (DAG) (4). IP_3 triggers the release of Ca^{2+} from stores in the endoplasmic reticulum, while DAG activates members of the protein kinase C (PKC) family. Following activation of stored Ca^{2+} by IP_3, influx of extracellular Ca^{2+} across the plasma membrane may further contribute to an increase in $[Ca^{2+}]_i$, which is regulated by several Ca^{2+} pumps and buffers (1). The net level and duration of these Ca^{2+} signals regulate cellular responses, including transcription, apoptosis, endocytosis, chemotaxis, and metabolism (3).

Simultaneous stimulation of two GPCRs coupled to different Gα subunits, often Gαi or Gαs in combination with Gαq, has been shown to yield synergistic Ca^{2+} responses in several model systems (reviewed in (5)). Limited studies have demonstrated this synergy in primary cells, including neurons and platelets, but the mechanisms of synergy vary and are not well defined (6,7).

Synergistic Ca^{2+} responses resulting from heterologous GPCR ligation have been little studied in macrophages, where members of the GPCR superfamily can stimulate an increase in $[Ca^{2+}]_i$ by activating members of the PLCβ family (4). As part of a systematic screen of RAW264.7 macrophage cells, C5a and UDP demonstrated synergy in producing a rise in $[Ca^{2+}]_i$ (http://www.signaling-gateway.org/data/cgi-bin/table2.cgi?cellabbr=RW) (8)). C5a is an important inflammatory mediator for macrophages and UDP, which is released following cell damage, is also present at sites of

injury or infection (9,10). Both ligands signal through GPCRs; C5a signals through C5aR (11), and UDP signals through P2Y6 receptors (12). To examine GPCR cross-talk by these ligands in mouse macrophages we studied both RAW264.7 cells and primary bone marrow-derived macrophages (BMDMs)

Our studies show that signals generated by C5a and UDP, acting through Gαi- and Gαq-coupled pathways respectively, converge at the level of PLCβ, and that these ligands, both individually and in concert, selectively use one PLCβ isoform, PLCβ3, to activate the production of IP_3 and the consequent release of Ca^{2+} from intracellular stores.

EXPERIMENTAL PROCEDURES

Reagents. UDP, UTP, LPA, PAF, human C5a, and FITC-dextran were from Sigma-Aldrich. Mouse IgG_{2a} was from BD Pharmaceuticals. $F(ab')_2$ fragment of goat anti-mouse IgG was from Jackson Immunoresearch Inc. Anti-PLCβ3 was from P. Sternweis, UTSW. Anti-P-Akt and anti-P-ERK were from Cell Signaling Technologies. Fura2 was from Molecular Probes. Ionomycin, thapsigargin, pertussis toxin, LY294002, wortmannin, Calphostin C, staurosporine, U-73122, and U-73343 were from Calbiochem. Additional detailed protocols for reagents, procedures, and solutions are available on the internet (www.afcs.org and www.signaling-gateway.org) and are referenced according to protocol number (eg. PP00000226).

Culture of RAW264.7 cells is described in protocol PP00000226. Following lentiviral infection, positive transductants were selected by antibiotic resistance conferred by the particular viral construct used (PP00000206). These included puromycin (2 μg ml), G418 (100-500 μg/ml), hygromycin (50 μg/ml), and zeocin (100 μg/ml). Detailed specifications for each medium are available at http://www.signaling-gateway.org/data/cgi-bin/Protocols.cgi?cat=3.

Mice and culture of BMDM. Mice genetically deficient in Gαq, Gα11, PLCβ3, PLCβ4 or PLCβ2 were previously described (13-19). All strains were on the C57BL/6 background except PLCβ2-deficient mice, which were on 129SV. Genetically deficient and corresponding wild-type (wt) strains were bred and housed under approved animal protocols. For BMDM culture femurs and tibias were removed from sex- and age-matched mice (4-20 weeks of age, matched +/- 4 weeks) (PP0000017200). Briefly, marrow was flushed from bones, erythrocytes were lysed, and the white cells were seeded in non-tissue culture Petri dishes for selection by growth and adhesion. After 6 days, over 99% of the surviving cells were macrophages, and these cells were maintained for up to 35 days in culture. Cells were cultured overnight in tissue culture (TC) plates prior to use in assays.

Lentivirus-mediated RNAi. Lentivirus was produced with a combination of three plasmids: (i) pCMVΔR8.91 packaging plasmid, (ii) pMD.G envelope plasmid (20,21), and (iii) a lentiviral vector plasmid (http://www.signaling-gateway.org/data/plasmid). The packaging and envelope plasmids were generously provided by D. Trono, Geneva. The lentiviral vector plasmids contained shRNA sequences expressed under RNA polymerase III promoters (U6 or H1) upstream of a Ubi-C promoter driving bicistronic expression of either EGFP or an hCD4 marker, followed by a resistance gene for either puromycin or hygromycin (22). Transfection of the 3 plasmids into 293T cells utilized lipofectamine 2000 (Invitrogen) and 20 μg of total DNA in a ratio of 4:3:2 for vector, packaging, and envelope plasmids respectively (PP00000200). Two days post-transfection, lentivirus was concentrated by using Centricon microfiltration tubes (PP00000202). Macrophages were infected at a multiplicity of infection of ~10 in the presence of polybrene at 4 μg/ml (PP00000215) (22). shRNAs targeting murine PLCβ2, PLCβ3 and PLCβ4 employed the sequences GAA CAG AAG TTA CGT TGT C, GCA GCG AGA TGA TTT GAT T, and ACG CGA TTG AGT TTG TAA ATT A, respectively.

Retrovirus-mediated transduction of macrophages with PLCβ. pFB-neo vectors carrying YFP-tagged murine PLCβ3 or YFP-FLAG epitope were transfected into the PlatE packaging line (23) to produce ecotropic retroviruses for transduction of day-2 cultures of bone marrow cells, which were differentiated into BMDM as described above.

Population calcium assays. Ca^{2+} responses were measured by monitoring the fluorescence of Fura-2-loaded cells (PP00000211). Baseline readings were collected for 30-40 sec. Calibration steps included additions of a Ca^{2+}-minimizing solution (PS00000607) and Fura-2 Ca^{2+}-saturating solution (PS00000608) at the end of each recording, to allow calculation of $[Ca^{2+}]_i$ values according to the method of Grynkiewicz (24), assuming a cytoplasmic K_d of 250 nM for Fura-2. Ca^{2+} signals during the response period were quantified by features as indicated, including the peak offset response

(difference between baseline Ca^{2+} level and the maximal Ca^{2+} level observed, reported in nM) and an integrated response (integrated Ca^{2+} level above the average baseline over the indicated time period, reported in nM x seconds).

Single-cell calcium assays. BMDM were plated in chambered coverglasses (Nunc, 8 wells/coverglass), cultured overnight, and loaded with Fura-2-AM as described above. Video microscopy was performed on a Nikon TE-300 fluorescence microscope equipped with a Photometrics HQ2 camera, 37°C stage incubator (Bionomics), Xe lamp (Sutter), and filter/shutter/dichoric controllers (Sutter and Conix). SimplePCI software was used to control collection parameters and extract fluorescence intensity data for individual cells.

IP_3 assay. After cell culture overnight, cells were placed in serum-free medium containing, 0.01% BSA. After 1 hr, ligands were added and, after varied time periods, dishes were transferred to ice, the media aspirated, and the cells washed with cold PBS. Cells were scraped into 125 µl of 5.4% perchloric acid solution and transferred to siliconized microfuge tubes on ice. Samples were centrifuged at 14,000xg for 15 min at 4°C. 120 µl of supernatant was neutralized with 5 N KOH containing 60 mM HEPES, and the samples were recentrifuged at 14,000xg for 15 min at 4°C. The IP_3 content of the final supernatant was assayed with an Amersham IP_3 [^{3}H] Biotrak assay kit. Results were reported as pmoles IP_3 per 10^6 cells.

SDS-PAGE and Western blot analysis of phosphoproteins (protocols PP00000168 and PP00000181). Cells were stimulated under the same conditions used for the IP_3 assay. Then buffer was aspirated, the cells were scraped into Laemelli sample buffer, and the samples were heated. SDS-PAGE gels were loaded with 20 µg protein per lane, and Western blots were probed with anti-P-Akt, anti-P-ERK, and anti-Rho-GDI. Fluorescent signals, measured for P-Akt and P-ERK by using a phosphoimager, were normalized to Rho-GDI.

Macropinocytosis assay. Macropinocytosis was assessed by measuring the cellular uptake of fluorescently labeled FITC-dextran. In brief, BMDM cells were cultured overnight in non-TC plates. Medium was replaced with Hank's Balanced Salt Solution with 1 mg/ml BSA, pH 7.4. After 1 hr ligands were added together with FITC-dextran (150 KDa MW, Sigma, 1 mg/ml final concentration in well). Activity was stopped with cold medium. After washing, cells were harvested in PBS with 5 mM EDTA and 5 mg/ml BSA, and analyzed by flow cytometry (FACSCalibur, BD) in 0.4% trypan blue solution (Sigma) to quench extracellular fluorescence. Ligand-stimulated activity was expressed as a ratio ('fold stimulation') to baseline activity.

Statistical Analyses. The error bars in graphs depict the standard error of the mean. The statistical significance of each comparison was evaluated by performing Student's t-tests for one-way analysis of variance, followed by Dunnett or individual t-tests (with Bonferroni correction), or non-linear mixed effects modeling, as appropriate. The effects of RNAi on Ca^{2+} responses in RAW264.7 cells were analyzed by non-linear mixed-effects modeling because of the non-normal distribution of Ca^{2+} response features, and because of variation in responses between cell lines and assays. A p-value of <0.05 was considered significant.

RESULTS

UDP and C5a interact to produce a synergistic calcium response in macrophages. As part of a large-scale screen, we observed a synergistic interaction between UDP and C5a for Ca^{2+} signaling (http://www.signaling-gateway.org/data/cgi-bin/table2.cgi?cellabbr=RW). This response showed a faster rise time and an increased peak-offset (peak response minus baseline) compared to the predicted additive response by the individual ligands (Fig. 1A). For the peak offset, the observed dual-ligand response was increased by 1.5 to 2-fold over the predicted additive response. Integration of the response over the first 20 sec yielded similar values. The ratio of observed/predicted values for such features of the response was referred to as the synergy ratio. BMDM showed a similar synergistic increase in the Ca^{2+} response, but the synergy ratio was much greater than in RAW264.7 cells (Fig. 1B).

For both cell types the optimal synergistic concentrations of each ligand were at or near the threshold for stimulation (Fig. 1C for BMDM, RAW264.7 data not shown). Synergy was nonetheless still observed at higher concentrations of both ligands, which fell within the linear portions of their dose-response curves. For RAW 264.7 cells, optimal concentrations for synergy were 0.25-100 nM C5a and 40-500 nM UDP, while for BMDM they were 0.1-3 nM C5a and 150-500 nM UDP.

Synergy is dependent on signaling through both Gαi- and Gαq- dependent GPCRs. C5a engages C5aR, which signals predominantly through Gαi-coupled heterotrimers (11,25,26). Thus, in BMDM and in RAW264.7, the Ca^{2+} response to C5a was inhibited following

treatment with pertussis toxin (Ptx), whereas that of UDP was not (Fig. 2A and supplemental Fig. S1). Ptx-mediated inhibition of signaling by low concentrations of C5a (<1 nM) was complete, but at high concentrations residual Ptx-insensitive calcium signaling was detected both in WT BMDM and in BMDM from mice lacking either Gαq or Gα11 (data not shown). Saturation of Ptx-intoxication of the C5a Ca^{2+} response was reached using 5 ng/ml for 18 hr, (supplemental Fig. S1) Others have demonstrated a role for Gα15 in C5a signaling in primary macrophages (27). While our data indicate that most C5a signaling is Ptx-sensitive, they are consistent with some signaling through Gα15 when C5a is present in high concentration. The Ca^{2+} response to C5a in BMDM from mice genetically deficient in Gαi2 was intact (data not shown), suggesting that Gαi3 is sufficient to support C5a signaling in these cells, since Gαi1 and Go are not expressed in macrophages (data not shown). Inhibition by Ptx was similar to that observed for WT cells (data not shown).

UDP binds to purinergic receptors of the P2Y family, which usually signal through members of the Gαq family (12,28,29). In accord with this, we found, that the Ca^{2+} response was completely lost in BMDM from Gαq-deficient mice (Fig. 2B). Surprisingly, although BMDM express other members of the Gαq family, including Gα11 and Gα15 (Fig. 2C), these are evidently unable to substitute for Gαq in the response to UDP. Further, the BMDM from Gα11-deficient mice had no reduction in Ca^{2+} responses for UDP (or for C5a, data not shown) compared with wildtype.

UDP only binds with high affinity to the P2Y6 receptor on macrophages. UTP, which has much lower affinity for P2Y6, binds also to P2Y2 and P2Y4 receptors (12,28). To demonstrate that the responses to UDP did not involve contaminating UTP, we separately tested UTP and UDP before and after treatment with hexokinase (12), which catalyzes conversion of UTP to UDP. Hexokinase treatment of UDP had no effect on its capacity to increase $[Ca^{2+}]_i$ in BMDM (not shown), indicating that contaminating UTP was not responsible for the observed responses in BMDM. The efficacy of hexokinase treatment was confirmed by showing that hexokinase treatment of UTP ablated its capacity to increase $[Ca^{2+}]_i$ in NIH 3T3 cells, which respond to UTP but not UDP

The removal of either Gαq or Gαi, via genetic deletion or Ptx intoxication, respectively, also eliminated any synergistic Ca^{2+} response to dual ligand stimulation (Fig. 2D). Thus, synergy between C5a and UDP is dependent on the Gi and Gq-linked subunit effectors that are activated by C5a and P2Y6 receptors, respectively.

Lysophosphatidic Acid (LPA) and platelet activating factor (PAF) also synergize with C5a for Ca^{2+} responses. To determine whether synergy for Ca^{2+} signaling occurred with other ligand pairs, we also examined responses to C5a or UDP in combination with PAF or LPA, both of which induce a Ca^{2+} response in macrophages through GPCRs. Pairing of C5a with either PAF or LPA demonstrated a robust synergy in Ca^{2+} signaling. Little or no synergy was seen with UDP/PAF, UDP/LPA or PAF/LPA (data not shown). The levels of synergy observed for C5a paired with LPA or PAF (Fig. 3A and B) were comparable to those for C5a paired with UDP.

PAF and LPA, like UDP, signaled Ca^{2+} primarily through Gαq in BMDM (Fig. 3C), but unlike UDP this was not exclusive; in the Gαq-deficient cells residual Ca^{2+} responses for PAF were abrogated by Ptx, indicating a minor contribution from Gαi-coupled pathways. Ptx did not reduce the Ca^{2+} response to LPA, but instead surprisingly enhanced it in both Gαq-deficient and wt BMDM (Fig. 3D). These data suggest for the first time that Gαi-coupled receptors basally inhibit LPA Ca^{2+} signaling. As with UDP, synergy by either LPA or PAF with C5a was lost in Gαq-deficient BMDM (data not shown). Thus, although these receptors can activate some Ca^{2+} signaling independently of Gαq, synergy with C5a nonetheless requires Gαq activation.

Overall, these results indicate that the simultaneous activation of Gαq and Gαi heterotrimers results in a synergistic Ca^{2+} response in macrophages. C5aR was the only endogenous Gαi-coupled GPCR on BMDM that we found to be capable of generating a robust Ca^{2+} response independently, and it was also the only receptor that synergized with ligands for Gαq-coupled receptors.

Synergy requires dual receptor occupancy. We next examined the possibility that one ligand might prime cells for subsequent responses, for example by increasing the supply of PIP_2 to provide a heightened state of responsiveness to the second stimulus (30). Although synergy was greatest when C5a and UDP were added simultaneously, it was also evident when ligands were added as much as 10 min apart. The sequence of addition was irrelevant. Fig. 4A shows the results for ligands separated by 100 sec. However, removal of the first ligand during the interim eliminated synergy (Fig. 4B). Thus,

if either ligand primes the synergistic response, this effect is rapidly lost. Functionally, synergy requires simultaneous receptor occupancy by both ligands.

Synergy affects the initial release of Ca^{2+} from intracellular stores and IP_3 production. Synergy between C5a and UDP affected the early rise in $[Ca^{2+}]_i$, suggesting an effect on the release of intracellular calcium stores. To test this, the Ca^{2+} responses to C5a and UDP, either alone or in combination, were measured after acute addition of EGTA to deplete extracellular Ca^{2+}. Synergy occurred in the presence of EGTA, confirming an effect on the release of intracellular Ca^{2+} (Fig. 4C). Without EGTA, however, synergy also extended to the sustained phase response, which is dependent on the influx of extracellular Ca^{2+}. Thus, synergy between C5a and UDP begins with the release of intracellular Ca^{2+} stores but extends to the influx of extracellular Ca^{2+}.

The release of Ca^{2+} from intracellular stores is activated by IP_3 binding to IP_3 receptors on the endoplasmic reticulum to open ER calcium channels (1). Simultaneous stimulation of BMDM with C5a and UDP in amounts that produced a synergistic Ca^{2+} response also resulted in synergy in the production of IP_3 (Fig. 4D), suggesting synergistic mechanisms are manifest at the level of PLCβ activation. Levels of IP_3 measured at 30 sec and 1 min after ligand additions were increased. Ca^{2+} levels began to decline while IP_3 was still rising, indicating that levels of $[Ca^{2+}]_i$ are not solely regulated by levels of IP_3.

The synergistic Ca^{2+} response is independent of feedback pathways involving PI3-kinase (PI3K) or PKC. Downstream of GPCR activation, PLCβ may be regulated by other signaling components, including those generated following the activation of PI3K (by Gβγ subunits) or of PKC (by DAG) (5). In our studies, however, inhibition of PI3K by LY294002 or of PKC by Calphostin C or staurosporine did not significantly affect synergy (supplemental Fig. S2.). The activity of the inhibitors was confirmed by inhibition of Akt or MARCKS phosphorylation (supplemental Fig. S3) These data are further evidence that an early signaling event is involved in the mechanism of synergy.

C5a and UDP make selective use of PLCβ isoforms. To examine the role of PLCβ in the signaling response to C5a and UDP, we first determined levels of transcripts for PLCβ isoforms in RAW264.7 cells and in BMDMs. By both microarray analysis (data not shown) and by RT-PCR (Fig. 5), we found that both cell types express PLCβ2, PLCβ3, and PLCβ4, with little or no PLCβ1. At the transcript level, the proportions of these PLCβ isoforms, however, differ between RAW264.7 cells and BMDM; normalized to PLCβ3, RAW264.7 cells express similar levels of transcripts for PLCβ2, PLCβ3 and PLCβ4, while BMDM express PLCβ2 >PLCβ3 >PLCβ4.

To determine if C5a and/or UDP made selective use of these PLCβ isoforms, we examined the Ca^{2+} response in BMDM from mice genetically deficient in PLCβ2, PLCβ3, or PLCβ4. BMDM from mice deficient in PLCβ3 demonstrated a marked loss of signaling in response to all GPCR ligands, including, C5a, UDP, PAF and LPA (Fig. 6 and Table1). Activation of Ca^{2+} responses, however, was intact in response to ligation of FcγRI by crosslinked IgG2a (Fig. 6), demonstrating that macrophages from PLCβ3-deficient mice are not deficient in the generation of $[Ca^{2+}]_i$ to a non-GPCR ligand. In BMDM from mice deficient in PLCβ4, the Ca^{2+} response to UDP was also consistently reduced, while the response to C5a was slightly elevated (Table 1, Fig. 6) and FcγRI signaling was normal. No loss of signaling to either UDP or C5a was seen in BMDM from mice deficient in PLCβ2. Thus, in BMDM, signaling by both C5a and UDP is selectively dependent on PLCβ3, but signaling by UDP is also partly dependent on PLCβ4.

To examine the role of PLCβ in RAW264.7 cells, we used RNAi against the different PLCβ isoforms. The loss of PLCβ isoforms in response to RNAi was incomplete (supplemental Fig. S4), but this approach allowed the testing of a uniform cell line, and it avoided possible developmental effects on macrophages due to PLCβ isoform loss. The depletion of PLCβ3 from RAW264.7 cells by RNAi reduced signaling by C5a, though not to the same extent as in BMDM genetically deficient in PLCβ3 (Table 2). Cells depleted of PLCβ3 by RNAi were not deficient in their response to UDP, but RNAi against PLCβ4, caused a loss of signaling in response to UDP, with a slight elevation in C5a signaling (Table 2). Thus, signaling by C5a depends mostly on PLCβ3 in both BMDM and RAW264.7 cells. Signaling by UDP is partially dependent on PLCβ3 in BMDM, but we could not detect this dependency in RAW264.7 cells by RNAi of PLCβ3. Signaling by UDP is also dependent on PLCβ4 in both BMDM and RAW264.7 cells, while deficiency of PLCβ4 augments C5a signaling in both cells.

Ca^{2+} responses are restored in PLCβ3-deficient BMDM reconstituted with PLCβ3. Retroviruses were used to transduce wildtype

and PLCβ3-deficient BMDM with either YFP-tagged murine PLCβ3 or control YFP-tagged FLAG cDNAs. Single-cell calcium assays were performed, which allowed identification of transduced cells by YFP fluorescence and comparison of responses by transduced and non-transduced cells (Fig. 6 B, C). Reconstitution of PLCβ3-deficient BMDM with PLCβ3 reconstituted the Ca^{2+}response to both C5a and UDP, alone and in combination, indicating that the loss of Ca^{2+} response in the PLCβ3-deficient cells is not due to an associated developmental defect.

Synergistic Ca^{2+} responses also show isoform dependence. We next tested the role of the PLCβ isoforms in synergy between C5a and UDP. In BMDM lacking PLCβ3 or PLCβ4, only those deficient in PLCβ3 were deficient in synergy (Fig. 7A and Table 3), as reflected by a reduced synergy ratio. Because signaling by individual ligands was lower than wildtype in these cells, the predicted additive responses were also lower, but a residual synergistic response was still detected in PLCβ3 deficient cells (Table 3). Thus synergy in Ca^{2+} signaling, like signaling by individual ligands, is primarily dependent on PLCβ3, but some synergy can be seen without it, Notably, lack of PLCβ4 did not reduce synergy in BMDM but instead enhanced it. We conclude that PLCβ3, but not PLCβ4, plays an important role in synergy between these ligands as well as in their individual responses.

As with Ca^{2+} signaling, BMDM lacking PLCβ3, but not PLCβ4, failed to demonstrate synergy in the production of IP_3 (Fig. 7B). Thus, studies of both Ca^{2+} and IP_3 indicate that synergy in signaling by C5a and UDP is the result of enhanced activity of PLCβ3.

Dual-ligand effects on PI3-kinase contrast to those on PLC. In order to determine if the synergistic effects of C5a plus UDP dual ligand stimulation were reflected in signaling events other than PLC activation, we examined activation of PI3K. Gβγ subunits directly activate PI3K-p110γ (31) and GPCRs can also activate PI3K-p110α and PI3K-p110β (32). The Gαq subunit does not activate PI3K, but instead can interact with and inhibit PI3K-p110α (33,34). Thus, PI3K activity reflects important proximal GPCR signals. To assess activation of PI3K, we measured the phosphorylation of Akt, which requires anchoring of its PH domain to PIP_3 produced by PI3K at the cell membrane. In BMDM, C5a rapidly activated PI3K, with peak phosphorylation of Akt at ~3 min (data not shown). In contrast, UDP did not activate PI3K, and it inhibited the phospho-Akt response to C5a (Fig. 8). This inhibition of Akt phosphorylation by UDP was at least partially selective, as ERK phosphorylation showed additivity. UDP did not inhibit PI3K activation in response to the crosslinking of FcγRI (data not shown), demonstrating that signaling by UDP did not globally interfere with all forms of PI3K activation. The observation that UDP inhibits PI3K activation by C5a while promoting Ca^{2+} signaling suggests that these pathways are differentially regulated.

The opposing effects of C5a/UDP signal-interactions on PLC and PI3K are reflected in macropinocytosis. Macropinocytosis, the endocytic process whereby cells internalize substantial volumes of extracellular fluid and solutes, is dependent on both PLC and PI3K (35,36), and this 'sampling' of the environment contributes to macrophage antigen presentation (37,38). We found that C5a activates macropinocytosis by BMDM, while UDP does not. Macropinocytosis was inhibited by dual-ligand stimulation (Fig. 9), in contrast to synergy for PLC and Ca^{2+} but in parallel with the inhibition of PI3K.

DISCUSSION

Our studies demonstrate the preferential use of PLCβ isoforms by GPCRs in eliciting a Ca^{2+} response in macrophages. Further, they indicate that synergy in signaling by the Gαi-coupled C5aR, together with the Gαq-coupled P2Y6 receptor for UDP, depends on a selective use of PLCβ3. Synergy in the Ca^{2+} response to C5a and UDP correlated with synergy in IP_3 production, suggesting signal convergence at the level of PLCβ activation. In contrast to Ca^{2+} activation, synergy between C5a and UDP was not observed in PI3K activation. Instead, the activation of PI3K by C5a was opposed by UDP. A similar effect was seen in the activation of macropinocytosis, which is dependent on both PLC and PI3K. Thus, synergy was selective for IP_3 production and the Ca^{2+} response, consistent with a selective effect on PLCβ.

The preferential use of PLC isoforms by GPCRs in macrophages did not simply reflect differential levels of expression of transcripts for the PLCβ isoforms. Four isoforms of PLCβ have been identified (4). We found that both BMDM and RAW264.7 cells expressed transcripts for PLCβ2, β3 and β4 but not PLCβ1, as determined by gene array analyses on Affymetrix chips and by RT-PCR. We have not been able to develop assays that adequately quantify differences in protein expression of these PLCβ isoforms, but our results nonetheless suggest that the selective use of PLCβ3 in

macrophages for Ca^{2+} signaling and synergy is despite the expression of PLCβ2 and PLCβ4. Thus, in contrast to platelets and neutrophils, PLCβ3 appears to be the major functional isoform in macrophages. While this paper was in preparation, Wang et al, also reported reduced Ca^{2+} responsiveness to C5a by macrophages from PLCβ3-deficient mice, and they linked this to increased apoptosis, and diminished atherosclerosis (39). Our studies demonstrate that in macrophages UDP can use PLCβ4 as well as PLCβ3, but C5a synergizes with UDP and other activators of Gαq through signals that converge at the level of PLCβ3, and responsiveness can be restored by transduction of cells with PLCβ3, showing that the defect in signaling does not reflect developmental changes in other pathways.

Synergy in the macrophage Ca^{2+} response was observed both in the initial, rapid release of Ca^{2+} from intracellular stores and in the sustained elevation of cytoplasmic Ca^{2+} levels. This observation is important, as there are examples of ligand interactions that increase $[Ca^{2+}]_i$ only via the influx of Ca^{2+} through plasma membrane Ca^{2+} channels (40).

Synergy between Gαi- and Gαq-coupled receptors has previously been observed in other cell types. In several systems, including smooth muscles, astrocytes, and kidney epithelial cells, Gαi-coupled GPCRs may alone not trigger a Ca^{2+} response, but responses may be facilitated in combination with, or after priming by, Gαq-coupled receptors (41-43). This synergy is reflected in the generation of IP_3, as in our current studies of macrophages, implicating PLC in the pathway of synergy.

Our findings narrow the possible mechanisms by which synergy in Ca^{2+} signaling by macrophages may occur. All PLCβ isoforms can bind Gαq subunits, albeit with differing affinities (44-48), and under certain conditions PLCβ4 demonstrates the highest specific activity for hydrolyzing PIP_2 (49). Consistent with this, the absence of PLCβ4 reduced mobilization of $[Ca^{2+}]_i$ by all ligands that activate Gαq, including UDP, LPA, and PAF. The loss of PLCβ4, however, did not impair synergy but instead increased it. Thus, PLCβ4 appears to inhibit rather than promote synergy in macrophages. PLCβ2 and β3 are both potently activated by Gβγ (25,47,50,51), while PLCβ4 is not (49). Although most Ca^{2+} synergy was lost in mice lacking PLCβ3, we could still detect low levels of synergy. We hypothesize that PLCβ2 may be capable of mediating synergy, but in macrophages the contribution of PLCβ2 is small in relation to that of PLCβ3.

In all, these results suggest that synergy between C5a and UDP in Ca^{2+} signaling in macrophages does not require multiple isoforms of PLCβ but instead involves the convergence of molecular mechanisms that primarily activate PLCβ3, but which may to a lesser extent activate PLCβ2.

Synergy between the Gαi receptor C5aR and Gαq receptors, does not establish that Gαq itself participates in the synergy. Gβγ signaling may differ between C5a and UDP, and synergy could reflect interactions between their unique Gβγ pathways. Indeed, loss of Gβ2 subunits via RNAi disrupts C5a but not UDP Ca^{2+} responses in RAW264.7 cells ((52), and data not shown). .

In our studies, C5a synergized not only with UDP, but also with PAF and LPA in stimulating a rise in $[Ca^{2+}]_i$. Studies of Gαq-deficient BMDM confirmed that both PAF and LPA utilize Gαq, but they also revealed important and interesting differences between these ligands and UDP. Unlike UDP, neither PAF nor LPA was fully dependent on Gαq. The remaining Ca^{2+} signaling with PAF utilized Gαi, as interruption of this pathway with Ptx in the absence of Gαq removed all Ca^{2+} signaling in response to PAF. In contrast, LPA Ca^{2+} signaling was not reduced by Ptx. Instead it was markedly increased. The G proteins used by LPA to elevate $[Ca^{2+}]_i$ in Gαq-deficient BMDM are unknown, but it appears that they are normally inhibited by Gαi.

At high ligand concentrations, C5a also demonstrated some Ptx-insensitive activation of Ca^{2+} signaling. We found that this response was still present in Gαq- or Gα11-deficient mice, suggesting coupling of C5aR to the more promiscuous Gα15, as has been observed by others (27). However, no Ca^{2+} synergy was observed with the combination of two Gαq-family linked ligands. Optimal synergy was observed at low concentrations of C5a, where the C5a-stimulated Ca^{2+} response was entirely Ptx sensitive, so we infer that the synergy is attributable to the Gαi activation by C5aR. In BMDM, the C5a receptor was the only Ca^{2+} signaling receptor identified that was primarily dependent on Gαi.

GPCR-mediated PLCβ activation can be regulated by positive or negative feedback loops. The PH-domain of PLCβ preferentially binds to the phosphatidylinositiol-3-phosphate (PI3P) product of PI-3K (4) and thus PI3K has the potential to modulate PLCβ activity. In our studies, however, inhibition of PI3K by LY294002 did not alter the Ca^{2+} synergy, indicating that PI3K does not measurably contribute to synergy. PKC may interact with

PLC at several levels. It can directly phosphorylate PLCβ, inactivating it (53). It can also phosphorylate and regulate signaling via GPCRs, and can phosphorylate some G protein-coupled receptor kinases (GRKs) (54). In our studies, however, inhibition of PKC with either Calphostin C or staurosporine did not alter Ca^{2+} synergy.

The acute nature of the synergy observed (occurring within seconds of dual ligand addition) and the demonstrated requirement for simultaneous dual receptor occupancy argue against the possibility that one receptor might drive 'priming' events affecting responses to the second receptor. Mechanisms for synergy reflecting priming effects have been proposed in a number of other systems (55). The immediate synergy in macrophages precludes changes in receptor or other protein expression levels. Alternatively, a priming event could increase the supply of the PLC substrate PIP_2 to enhance production of IP_3 (56-58), and in some cases this has been shown to persist for hours after first ligand stimulation. This synergy mechanism would not require dual receptor occupation during heterologous ligand stimulations of Ca^{2+} unless increases in the supply of PIP_2 were lost rapidly (we tested 3 minutes after 1st ligand removal by which time synergy was lost).

The consequences of combined signaling by C5a and UDP in macrophages may be particularly important in areas of inflammation, where C5a is produced, and where UDP may be released from dying cells (59). C5a in particular plays a central role in inflammation, and consequences of Ca^{2+} signaling would be augmented by UDP, while consequences of PI3K activation would be inhibited. The recent report describing a reduction of atherosclerosis in PLCβ3-deficient mice, due to macrophage hypersensitivity to apoptotic induction, links inflammatory outcome to Ca^{2+} signaling and survival in macrophages (39).

REFERENCES

1. Berridge, M. J., Bootman, M. D., and Roderick, H. L. (2003) *Nat Rev Mol Cell Biol* **4**, 517-529
2. Carafoli, E., Santella, L., Branca, D., and Brini, M. (2001) *Crit Rev Biochem Mol Biol* **36**, 107-260
3. Feske, S. (2007) *Nat Rev Immunol* **7**, 690-702
4. Rhee, S. G. (2001) *Annu Rev Biochem* **70**, 281-312
5. Werry, T. D., Wilkinson, G. F., and Willars, G. B. (2003) *Biochem J* **374**, 281-296
6. Toms, N. J., and Roberts, P. J. (1999) *Neuropharmacology* **38**, 1511-1517
7. Abrams, C. S. (2005) *Curr Opin Hematol* **12**, 401-405
8. Natarajan, M., Lin, K. M., Hsueh, R. C., Sternweis, P. C., and Ranganathan, R. (2006) *Nat Cell Biol* **8**, 571-580
9. Hawlisch, H., Wills-Karp, M., Karp, C. L., and Kohl, J. (2004) *Mol Immunol* **41**, 123-131
10. Boeynaems, J. M., and Communi, D. (2006) *J Invest Dermatol* **126**, 943-944
11. Skokowa, J., Ali, S. R., Felda, O., Kumar, V., Konrad, S., Shushakova, N., Schmidt, R. E., Piekorz, R. P., Nurnberg, B., Spicher, K., Birnbaumer, L., Zwirner, J., Claassens, J. W., Verbeek, J. S., van Rooijen, N., Kohl, J., and Gessner, J. E. (2005) *J Immunol* **174**, 3041-3050
12. Del Rey, A., Renigunta, V., Dalpke, A. H., Leipziger, J., Matos, J. E., Robaye, B., Zuzarte, M., Kavelaars, A., and Hanley, P. J. (2006) *J Biol Chem* **281**, 35147-35155
13. Hashimoto, K., Watanabe, M., Kurihara, H., Offermanns, S., Jiang, H., Wu, Y., Jun, K., Shin, H. S., Inoue, Y., Wu, D., Simon, M. I., and Kano, M. (2000) *Prog Brain Res* **124**, 31-48
14. Offermanns, S., Hashimoto, K., Watanabe, M., Sun, W., Kurihara, H., Thompson, R. F., Inoue, Y., Kano, M., and Simon, M. I. (1997) *Proc Natl Acad Sci U S A* **94**, 14089-14094
15. Offermanns, S., Zhao, L. P., Gohla, A., Sarosi, I., Simon, M. I., and Wilkie, T. M. (1998) *Embo J* **17**, 4304-4312
16. Xie, W., Samoriski, G. M., McLaughlin, J. P., Romoser, V. A., Smrcka, A., Hinkle, P. M., Bidlack, J. M., Gross, R. A., Jiang, H., and Wu, D. (1999) *Proc Natl Acad Sci U S A* **96**, 10385-10390
17. Jiang, H., Lyubarsky, A., Dodd, R., Vardi, N., Pugh, E., Baylor, D., Simon, M. I., and Wu, D. (1996) *Proc Natl Acad Sci U S A* **93**, 14598-14601

18. Kano, M., Hashimoto, K., Watanabe, M., Kurihara, H., Offermanns, S., Jiang, H., Wu, Y., Jun, K., Shin, H. S., Inoue, Y., Simon, M. I., and Wu, D. (1998) *Proc Natl Acad Sci U S A* **95**, 15724-15729
19. Jiang, H., Kuang, Y., Wu, Y., Xie, W., Simon, M. I., and Wu, D. (1997) *Proc Natl Acad Sci U S A* **94**, 7971-7975
20. Salmon, P., Kindler, V., Ducrey, O., Chapuis, B., Zubler, R. H., and Trono, D. (2000) *Blood* **96**, 3392-3398
21. Rossi, G. R., Mautino, M. R., and Morgan, R. A. (2003) *Hum Gene Ther* **14**, 385-391
22. Fraser, I., Liu, W., Rebres, R., Roach, T., Zavzavadjian, J., Santat, L., Liu, J., Wall, E., and Mumby, M. (2006) *Methods Mol Biol* **365**, 261-286
23. Morita, S., Kojima, T., and Kitamura, T. (2000) *Gene Ther* **7**, 1063-1066
24. Grynkiewicz, G., Poenie, M., and Tsien, R. Y. (1985) *J Biol Chem* **260**, 3440-3450
25. Jiang, H., Kuang, Y., Wu, Y., Smrcka, A., Simon, M. I., and Wu, D. (1996) *J Biol Chem* **271**, 13430-13434
26. Sarndahl, E., Bokoch, G. M., Boulay, F., Stendahl, O., and Andersson, T. (1996) *J Biol Chem* **271**, 15267-15271
27. Davignon, I., Catalina, M. D., Smith, D., Montgomery, J., Swantek, J., Croy, J., Siegelman, M., and Wilkie, T. M. (2000) *Mol Cell Biol* **20**, 797-804
28. Di Virgilio, F., Chiozzi, P., Ferrari, D., Falzoni, S., Sanz, J. M., Morelli, A., Torboli, M., Bolognesi, G., and Baricordi, O. R. (2001) *Blood* **97**, 587-600
29. Erb, L., Liao, Z., Seye, C. I., and Weisman, G. A. (2006) *Pflugers Arch* **452**, 552-562
30. Stephens, L., Jackson, T. R., and Hawkins, P. T. (1993) *Biochem J* **296 (Pt 2)**, 481-488
31. Hazeki, O., Okada, T., Kurosu, H., Takasuga, S., Suzuki, T., and Katada, T. (1998) *Life Sci* **62**, 1555-1559
32. Thelen, M., and Didichenko, S. A. (1997) *Ann N Y Acad Sci* **832**, 368-382
33. Ballou, L. M., Lin, H. Y., Fan, G., Jiang, Y. P., and Lin, R. Z. (2003) *J Biol Chem* **278**, 23472-23479
34. Ballou, L. M., Chattopadhyay, M., Li, Y., Scarlata, S., and Lin, R. Z. (2006) *Biochem J* **394**, 557-562
35. Swanson, J. A., and Watts, C. (1995) *Trends Cell Biol* **5**, 424-428
36. Swanson, J. A., Yirinec, B. D., and Silverstein, S. C. (1985) *J Cell Biol* **100**, 851-859
37. Conner, S. D., and Schmid, S. L. (2003) *Nature* **422**, 37-44
38. Rock, K. L., and Shen, L. (2005) *Immunol Rev* **207**, 166-183
39. Wang, Z., Liu, B., Wang, P., Dong, X., Fernandez-Hernando, C., Li, Z., Hla, T., Claffey, K., Smith, J. D., and Wu, D. (2007) *J Clin Invest*
40. Dianzani, C., Lombardi, G., Collino, M., Ferrara, C., Cassone, M. C., and Fantozzi, R. (2001) *J Leukoc Biol* **69**, 1013-1018
41. Selbie, L. A., and Hill, S. J. (1998) *Trends Pharmacol Sci* **19**, 87-93
42. Werry, T. D., Wilkinson, G. F., and Willars, G. B. (2003) *J Pharmacol Exp Ther* **307**, 661-669
43. Werry, T. D., Christie, M. I., Dainty, I. A., Wilkinson, G. F., and Willars, G. B. (2002) *Br J Pharmacol* **135**, 1199-1208
44. Jiang, H., Wu, D., and Simon, M. I. (1994) *J Biol Chem* **269**, 7593-7596
45. Lee, C. H., Park, D., Wu, D., Rhee, S. G., and Simon, M. I. (1992) *J Biol Chem* **267**, 16044-16047
46. Jhon, D. Y., Lee, H. H., Park, D., Lee, C. W., Lee, K. H., Yoo, O. J., and Rhee, S. G. (1993) *J Biol Chem* **268**, 6654-6661
47. Smrcka, A. V., and Sternweis, P. C. (1993) *J Biol Chem* **268**, 9667-9674
48. Runnels, L. W., and Scarlata, S. F. (1999) *Biochemistry* **38**, 1488-1496
49. Lee, C. W., Lee, K. H., Lee, S. B., Park, D., and Rhee, S. G. (1994) *J Biol Chem* **269**, 25335-25338
50. Wu, D., Katz, A., and Simon, M. I. (1993) *Proc Natl Acad Sci U S A* **90**, 5297-5301

51. Park, D., Jhon, D. Y., Lee, C. W., Lee, K. H., and Rhee, S. G. (1993) *J Biol Chem* **268**, 4573-4576
52. Hwang, J. I., Fraser, I. D., Choi, S., Qin, X. F., and Simon, M. I. (2004) *Proc Natl Acad Sci U S A* **101**, 488-493
53. Yue, C., Ku, C. Y., Liu, M., Simon, M. I., and Sanborn, B. M. (2000) *J Biol Chem* **275**, 30220-30225
54. Ferguson, S. S. (2001) *Pharmacol Rev* **53**, 1-24
55. Yang, C. M., Chien, C. S., Wang, C. C., Hsu, Y. M., Chiu, C. T., Lin, C. C., Luo, S. F., and Hsiao, L. D. (2001) *Biochem J* **354**, 439-446
56. Schmidt, M., Lohmann, B., Hammer, K., Haupenthal, S., Nehls, M. V., and Jakobs, K. H. (1998) *Mol Pharmacol* **53**, 1139-1148
57. Schmidt, M., Nehls, C., Rumenapp, U., and Jakobs, K. H. (1996) *Mol Pharmacol* **50**, 1038-1046
58. Schmidt, M., Bienek, C., Rumenapp, U., Zhang, C., Lummen, G., Jakobs, K. H., Just, I., Aktories, K., Moos, M., and von Eichel-Streiber, C. (1996) *Naunyn Schmiedebergs Arch Pharmacol* **354**, 87-94
59. Riedemann, N. C., Guo, R. F., Bernacki, K. D., Reuben, J. S., Laudes, I. J., Neff, T. A., Gao, H., Speyer, C., Sarma, V. J., Zetoune, F. S., and Ward, P. A. (2003) *Immunity* **19**, 193-202

FOOTNOTES

We thank K. Rose Finley, Michael McWay, Christina Moon and Amanda Norton at the San Francisco VA Medical Center and Joelle Zavzavadjian, Jamie Liu, Leah Santat, Lucas Cheadle and Estelle Wall at Caltech for excellent technical assistance. This work was supported by National Institutes of Health Grant GM 62114.

The abbreviations used are: BMDM, bone marrow-derived macrophages; C5a, complement component 5a; DAG, diacyl glycerol; GPCR, G-protein-coupled receptor; GRK, G protein-coupled receptor kinase; IP_3, inositol-1,4,5-trisphosphate; LPA, lysophosphatidic acid; PAF, platelet activating factor; PIP_2, phosphatidyl inositol-4,5-diphosphate; PKC, protein kinase C; PI3K, phosphatidyl inositol 3-kinase; PLC, phospholipase C; Ptx, pertussis toxin; UDP, uridine 5'-diphosphate; UTP, uridine 5'-triphosphate

FIGURE LEGENDS

Table 1. Single-ligand Ca^{2+} responses in PLCβ isotype-deficient BMDM. BMDMs derived from 4-7 individual PLCβ-deficient (-/-) mice per isoform were subjected to Ca^{2+} assays for near maximal concentrations of several GPCR ligands: C5a (10 nM), UDP (2.5 μM), LPA (2.5 μM), and PAF (12.5 nM). Three to four assays per cell population & ligand were performed, with 3-4 replicate samples per assay. Responses were normalized to the matched WT BMDMs in each assay and the table reports the average response of each isotype -/- as a % of WT response. Values are shown for peak-offset and integration to 60 sec measurements of the Ca^{2+} responses. PLCβ3-deficient BMDM showed reduced responsiveness to four GPCR ligands but not following ligation of FcγRI (FCG). PLCβ4-deficient BMDM showed a reduced Ca^{2+} response phenotype for UDP only. * $p<0.05$, ** $p<0.005$.

Table 2. RNAi against PLCβ3 and PLCβ4 in RAW264.7 reduces Ca^{2+} responses to C5a and UDP respectively. RNAi against PLCβ isoforms in RAW264.7 cells was performed by lentiviral-mediated RNAi using shRNA encoding constructs. Control lines lacking only shRNA were prepared and analyzed in parallel with each RNAi line. Ca^{2+} assays were performed with C5a (30nM) and UDP (25 μM) and responses were quantified by peak offset and integration to 1 or 2.5 min after ligand addition. Values were normalized to responses of control lines in each assay, and results of replicate lines were pooled to present the average response as a percent of control. Results represent 2-5 lines per target with 3-4 assays per line and 3-4 samples per ligand per assay. * $p<0.05$, ** $p<0.01$.

Table 3. Ca^{2+} response synergy in PLCβ isotype-deficient BMDMs. BMDMs derived from individual PLCβ isotype-deficient mice were subjected to Ca^{2+} assays for synergy between C5a and UDP (0.75 nM + 500 nM). Peak-offset values from Ca^{2+} responses by Fura-2 loaded cells were normalized to corresponding controls in each assay. Data were pooled to report average values as a percent of control (%WT) for the individual ligands and corresponding predicted additive responses. Synergy observed was reported as a percent of the calculated additive Ca^{2+} response for each cell type. Data were from 6 or 4 independent lines for PLCβ3 or PLCβ4-deficient cells respectively, with 2-4 replicate assays per population and 3-4 samples per condition per assay. * $p<0.05$, ** $p<0.005$.

Fig 1. UDP and C5a produce a synergistic Ca^{2+} response in macrophages. Intracellular Ca^{2+} levels were calculated for Fura-2-loaded adherent macrophage populations from kinetic assays in 96-well plates. After 40 sec baseline readings, ligands were added and responses were monitored for 2.5 min. Each line in the graphs represents the average of 3-4 individual wells per assay and the error bars (SEM) are shown for the dual-ligand line in each graph. Synergy was evaluated by comparing the experimentally observed dual ligand responses to the predicted additive responses of the individual ligands. The dual-ligand response was quantified as the ratio of the observed/predicted additive responses and the term 'synergy ratio' was applied to the ratio of the peak offsets (PO = peak height – baseline).
A. RAW264.7 cells were stimulated with UDP (2.5 μM), C5a (10 nM) or simultaneous UDP and C5a . Synergy ratio = 1.38. This is a representative experiment of n=12 with similar results.
B. BMDM were stimulated with UDP (500 nM), C5a (0.37 nM) or simultaneous UDP and C5a. Synergy ratio = 2.62. This is a representative experiment of >25 with similar results.
C. Dose-response pattern for simultaneous UDP and C5a-stimulated Ca^{2+} responses quantified by synergy ratio. Ligand concentrations are expressed as log(nM). The optimal synergy ratio was at ~ 300 nM UDP + 0.3 nM C5a. The surface was interpolated from 84 individual experiments composed of 15 samples each.

Fig 2. Synergy Requires Gαq- and Gαi-heterotrimer subunit effectors. Intracellular Ca^{2+} responses were measured in Fura-2-loaded BMDMs.
A. C5a Ca^{2+} responses are mostly Ptx sensitive. BMDM cultured overnight with or without Ptx (100 ng/ml) were stimulated with different concentrations of C5a (0.33 to 10 nM), or a single concentration of UDP (2.5 μM), and the peak offset of the Ca^{2+} responses was determined. Shown is a representative experiment of 7 with similar results. Values are mean+/-SEM of 3-4 replicate samples per condition. * $p<0.01$.
B. UDP responses are Gαq-dependent. Wildtype (WT), Gαq heterozygote (+/-) and Gαq-deficient (-/-) BMDM were stimulated with either UDP (2.5 μM) or C5a (10 nM). Peak-offsets of responses are shown normalized to those of the wildtype cells from each experiment. Values are mean+/-SEM from 3 experiments. * $p<0.001$.
C. Quantitative RT-PCR for Gαq family isoforms q, 11, and 15 was performed on RAW264.7 cell and BMDM samples to determine relative prevalence. Transcript levels were normalized to those for Gαq for the same cell type. Data shown are mean +/- SEM from n=3 samples per cell.
D. Synergy following dual ligand stimulation requires both Gαq and Gαi subunits. Wildtype (WT) or Gαq-deficient (-/-) BMDM were stimulated with UDP (500nM), C5a (0.75 nM), or simultaneous UDP and C5a. WT cells were cultured overnight with or without Ptx (100 ng/ml). Data shown are from a representative experiment of 3-4 with similar results. Each line in the graphs represents the average of 3-4 individual wells in the assay.

Fig 3. LPA and PAF also show synergy with C5a in Ca^{2+} responses, and they couple mainly with Gαq. Intracellular Ca^{2+} responses were measured in Fura-2 loaded BMDMs. Each line in the graphs represents the average of 3-4 individual wells per assay.
A. BMDM were stimulated with C5a (0.25 nM), LPA (0.25 nM) or simultaneous C5a and LPA. Data shown are from a representative experiment of n=18 with similar results.
B. BMDM were stimulated with C5a (0.25 nM), PAF (0.3 nM) or simultaneous C5a and PAF. Data shown are from a representative experiment of n=17 with similar results.
C. WT or Gαq-/- BMDM were stimulated with UDP (10 μM), PAF (12.5 nM) or LPA (2.5 μM). Data shown are from a representative experiment of n=8-14 with similar results.
D. WT or Gαq-/- BMDM were cultured overnight with or without Ptx and then stimulated with PAF (12.5 nM) or LPA (2.5 μM). Data shown are from a representative experiment of 4-5 with similar results.

Fig 4. C5a and UDP produce synergistic Ca^{2+} responses when added serially, but synergy requires dual ligand receptor occupancy. Intracellular Ca^{2+} responses were measured in Fura-2-loaded BMDM. Each line in the graphs represents the average of 3-4 individual wells per assay.
A. Serial addition of stimuli to BMDM provides synergy. C5a (0.75 nM), UDP (500 nM) or HBSS were added at the first time point (arrow 1), and after a 100 sec delay UDP or C5a was added at the second time point (arrow 2). The first stimulus was not removed prior to addition of the second.
B. Serial stimulation of BMDM does not provide synergy if the first ligand is removed prior to addition of the second. Either UDP (500 nM) or HBSS was added to the cells and incubated for 2 min. The buffer was then left in the wells another 3 min or the buffer was removed, the cells washed, and fresh buffer replaced in the wells. Either C5a (0.75 nM), C5a + UDP (0.75 nM + 500 nM), or HBSS was then added to the wells (2^{nd} addition, arrow labeled "2", 5 min delay from 1^{st} addition, thus 3 minute delay after 1^{st} ligand removal for washed samples), and the results of the second response period are shown. The left panel depicts responses to the 2^{nd} stimulus when the first ligand remains. The right panel depicts responses to the 2^{nd} ligand in the absence of the 1^{st} ligand.
C. Synergy was observed in the release of Ca^{2+} from intracellular stores. Each line in the graphs represents the average of 3-4 individual wells per assay. HBSS or EGTA (2 mM) was added to assay wells 30 sec prior to C5a (0.75 nM), UDP (500 nM) or simultaneous C5a and UDP.
D. IP_3 responses of BMDMs. Cells were stimulated with C5a (10 nM), UDP (2.5 μM), or simultaneous C5a and UDP for 0, 30 sec, or 1 min and signaling was stopped by cell lysis in perchloric acid as described for IP_3 measurements. IP_3 was measured using a competitive binding assay for the IP_3 receptor and results are reported as pmol / 10^6 cells. Values shown are mean +/- SEM from n=5-10 samples per condition.

Fig 5. Selective use of the PLCβ3 and β4 isoforms in GPCR signaling in BMDM did not correlate with higher levels of expression. Quantitative RT-PCR for PLCβ isoforms 1, 2, 3, and 4 was performed on RAW264.7 cell and BMDM samples to determine relative prevalence. Transcript levels were normalized to those for PLCβ3 for the same cell type. Data shown are mean +/- SEM from n=3-4 samples per cell. Little to no expression of PLCβ1 mRNA was observed, as shown.

Fig 6. PLCβ isoform-dependence of Ca^{2+} responses.
A. Ca^{2+} responses for C5a, UDP, LPA and PAF are reduced in PLCβ3-deficient BMDM compared to wildtype, but only the UDP response is reduced in PLCβ4-deficient BMDM. Intracellular Ca^{2+} responses were measured in Fura-2-loaded BMDM. Cells were stimulated with near-maximal doses of the 4 ligands tested: C5a (10 nM), UDP (10 μM), LPA (2.5 μM) or PAF (12.5 nM), or by FcγR cross-linking (cells preloaded with 5 μg/ml IgG2a, then treated with 44 μg/ml $F(ab')_2$ antibody fragments of rabbit anti-mIgG). Each line in the graphs represents the average of 3-4 individual wells per assay. Representative experiments are shown for matched wildtype versus PLCβ3- or PLCβ4-deficient (-/-) cells from n=8-33 assays with similar results. Assays were performed on 12 PLCβ3-deficient and 4 PLCβ4-deficient BMDM cultures which were independently derived.
B. Expression of PLCβ3 in PLCβ3-deficient BMDM restores single-ligand Ca^{2+} responses. Single cell Ca^{2+} assays were performed on wildtype (WT) or PLCβ3-deficient BMDM transduced with retrovirus encoding YFP-FLAG or YFP-PLCβ3. Cells were stimulated with C5a (10 nM) and peak-offset features of the Ca^{2+} traces calculated. Responses by transduced cells were measured in multiple assays of each of 2 independent batches of infected BMDM. Values shown are mean +/- SEM from n=3-9 samples per condition. *$p<0.05$.
C. Expression of PLCβ3 in PLCβ3-deficient BMDM restores dual-ligand Ca^{2+} responses to levels observed in WT BMDM. Single cell Ca^{2+} assays were performed on wildtype (WT) or PLCβ3-deficient BMDM transduced with retrovirus encoding YFP-FLAG or YFP-PLCβ3. Cells were stimulated with C5a (0.75 nM), UDP (500 nM), or C5a+UDP, and the Ca^{2+} responses were measured by integration over 2.5 min. Responses by transduced cells were measured in multiple assays of each of 3 independent batches of infected BMDM. Values shown are mean +/- SEM from n=11-17 samples per condition. *$p<0.05$.

Fig 7. The synergistic Ca^{2+} response shows selective use of the PLCβ3 isoform. Matched wildtype (+/+) versus PLCβ3- or PLCβ4-deficient (-/-) BMDMs were assayed for their ability to reflect synergistic responses to C5a plus UDP.
A.Intracellular Ca^{2+} responses were measured in Fura-2-loaded BMDM. Each line in the graphs represents the average of 3-4 individual wells per assay. Cells were stimulated with C5a (0.75 nM), UDP

(500 nM) or both ligands. Data shown are from representative experiments of n=9-19 with similar results.
B. IP_3 production in PLCβ isoform-deficient BMDM. Cells were stimulated with C5a (10 nM), UDP (2.5 μM), or simultaneous C5a and UDP as indicated, and signaling was stopped by cell lysis at 1 min after stimulation. IP_3 was measured using a competitive binding assay for the IP_3 receptor, and results are reported as pmol / 10^6 cells. Data represent pooled results from 2-4 assays with 2 replicate samples per condition per assay. * $p<0.005$.

Fig 8. UDP and other Gαq-coupled ligands antagonize C5a stimulation of PI3-kinase.
Adherent BMDM were stimulated with C5a (10 nM), UDP (10 μM), LPA (2.5 μM), PAF (50 nM), C5a plus UDP, C5a plus LPA or C5a plus PAF. After 1 min of stimulation, the assay was stopped by sample lysis. Western blots were probed with specific antibodies and were quantified by using a phosphor-imager. Phosphoprotein values were normalized to levels of RhoGDI in the samples and then expressed as a fold-increase above the baseline level, represented by the average of control cell samples not stimulated with specific ligands. Data are shown for P-Akt and P-ERK from nine replicate experiments as mean+/-SEM. * $p<0.05$, ** $p<0.01$.

Fig 9. UDP inhibits C5a-stimulated macropinocytosis. BMDM were stimulated with or without C5a (0, 0.3, 0.75, 2.5 nM) in the presence or absence of UDP (0, 0.5, 2.5 μM) in assays of macropinocytosis. Uptake of extracellular FITC-dextran was assessed by cytometry and normalized to the positive control (C5a 0.75 nM) in each assay (arbitrary units, AU) for summary purposes. Values show the mean +/-SEM from 8 experiments (n=4-8 per condition).

Table 1.

Measure of Response	Ligand	BMDM WT	BMDM PLCβ2-/-	BMDM PLCβ3-/-	BMDM PLCβ4-/-
Peak offset	C5a	100	118±19	20±4**	104±6
	UDP	100	150±32	44±3**	81±6*
	LPA	100	109±13	24±4**	86±13
	PAF	100	136±4*	38±4**	94±3
	FCG	100	114±12	104±10	87±20
Integrated 60s	C5a	100	131±28	18±3**	105±5
	UDP	100	159±40	44±3**	73±6*
	LPA	100	98±10	28±5**	89±13
	PAF	100	142±9*	34±3**	94±9

Table 2.

RNAi Target	# Lines	C5a Peak Offset	C5a Intgrated 1m	C5a Integrated 2.5m	UDP Peak Offset	UDP Intgrated 1m	UDP Integrated 2.5m
PLCβ2	2	71	58	82**	104	78	104
PLCβ3	2	61*	46*	62*	107	110	111
PLCβ4	5	125**	115	111	97	95	88*

Table 3.

Peak Offset Response

BMDM	C5a (%WT)	UDP (%WT)	Calculated Additive (%WT)	Synergy Observed % of Calculated Additive
WT	100	100	100	264±33
PLCβ3-/-	25±11**	41±5**	34±5**	158±21*
PLCβ4-/-	103±5	61±5*	78±6*	315±38*

Figure 1

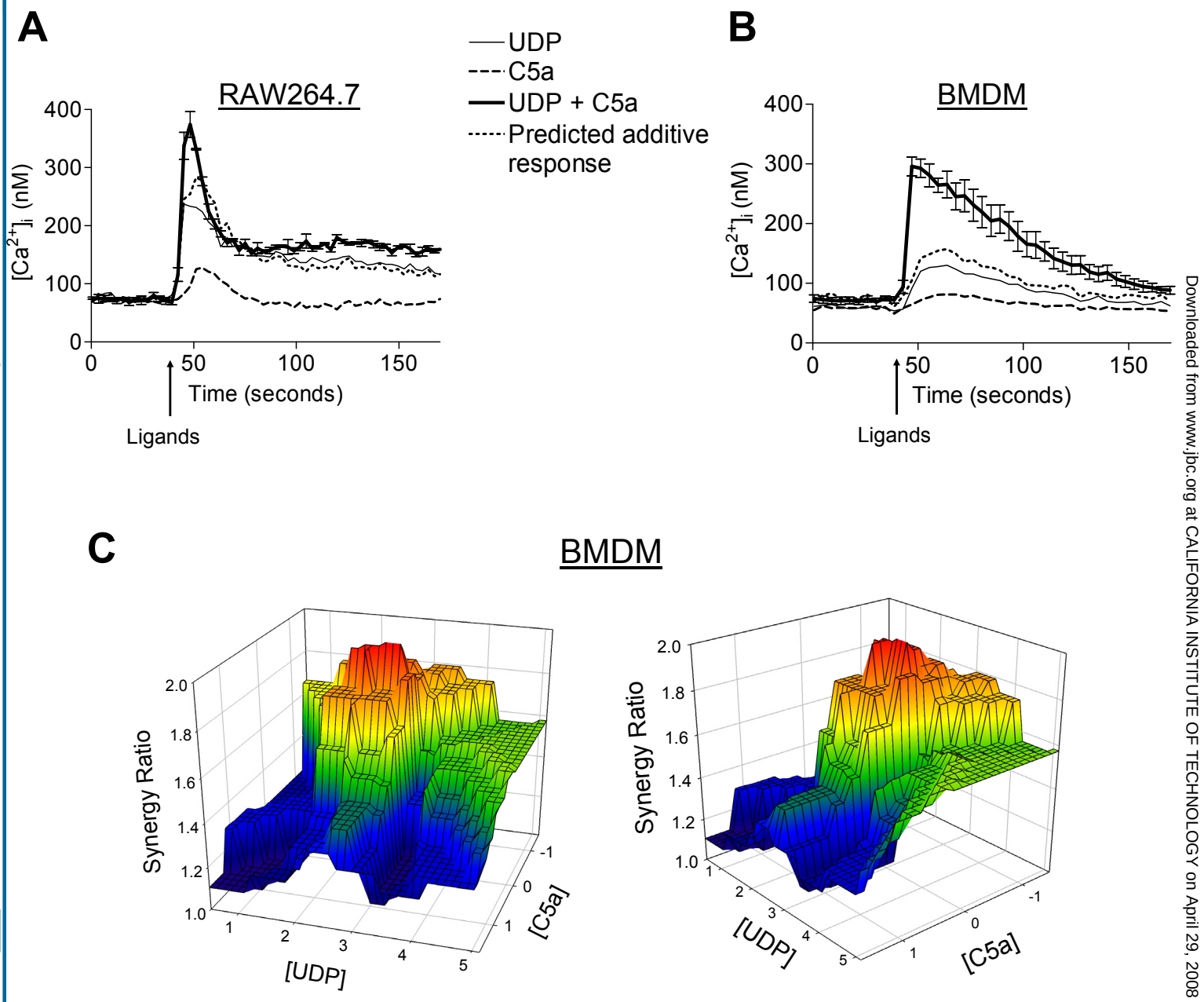

Figure 2

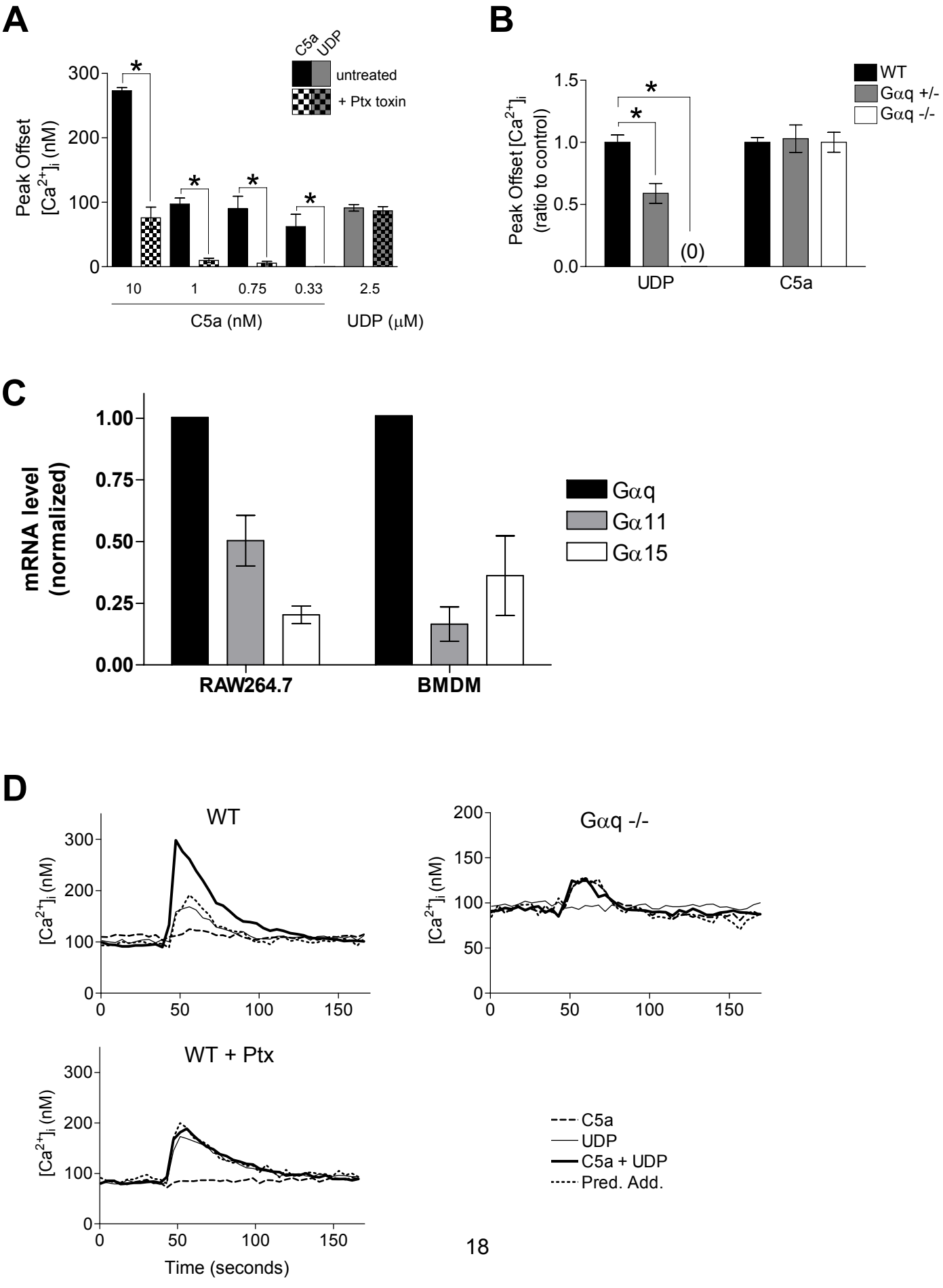

Figure 3

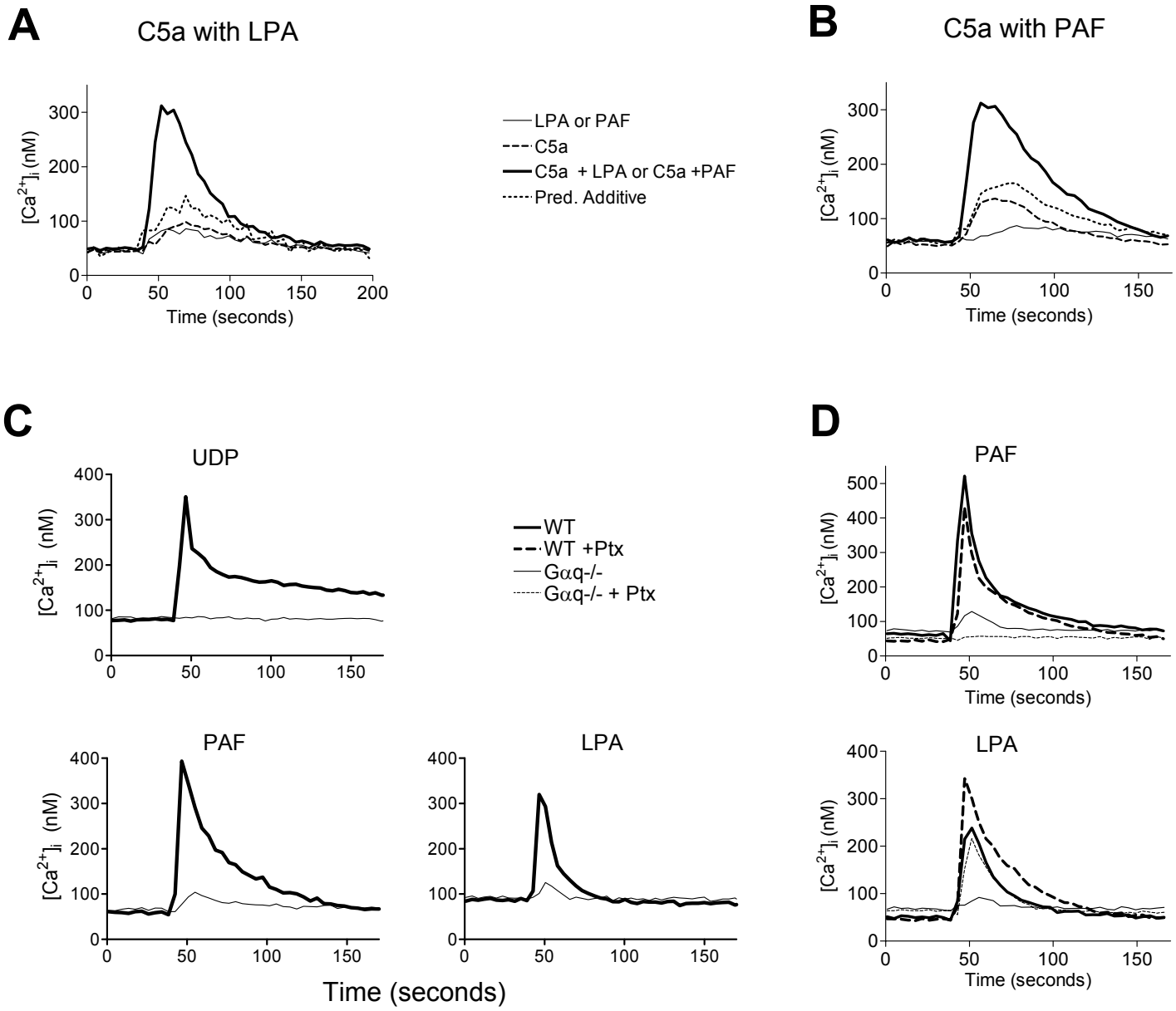

Figure 4

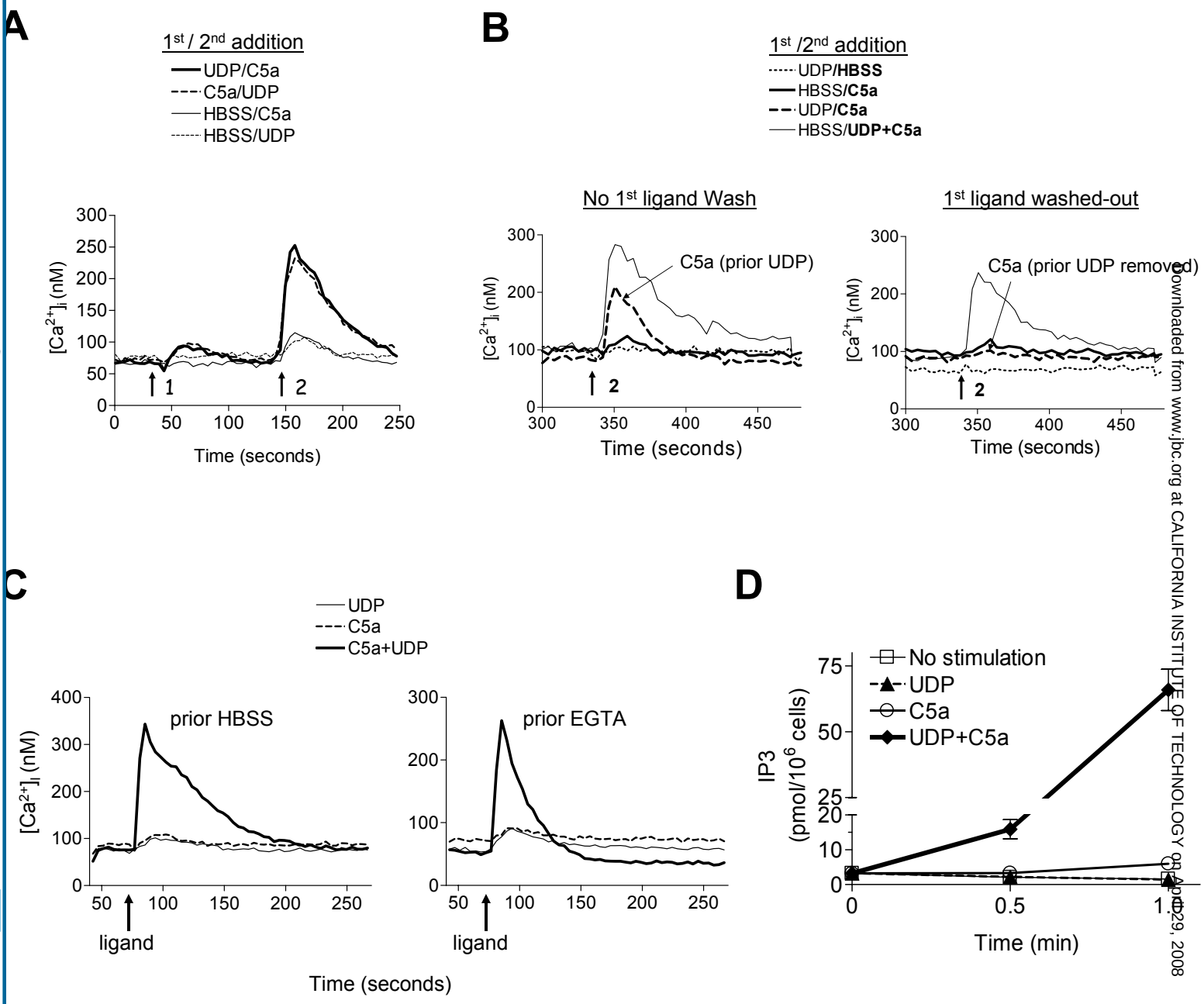

Figure 5

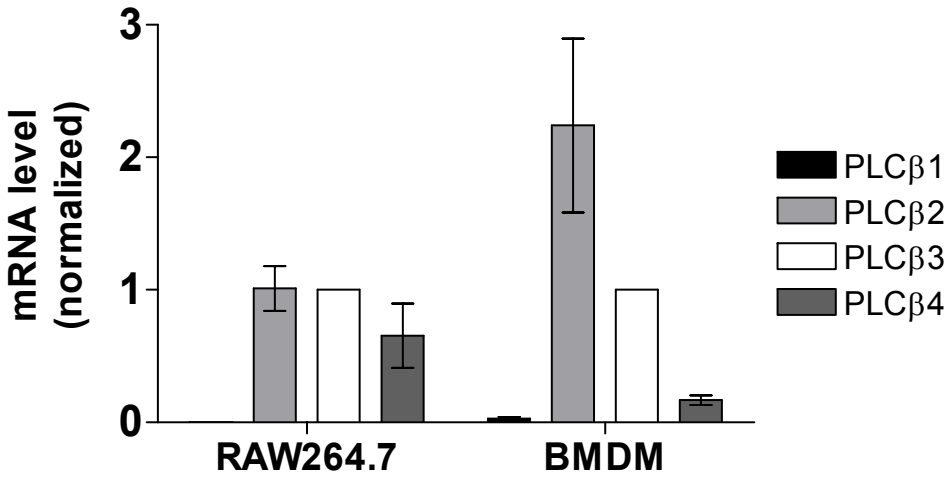

Figure 6

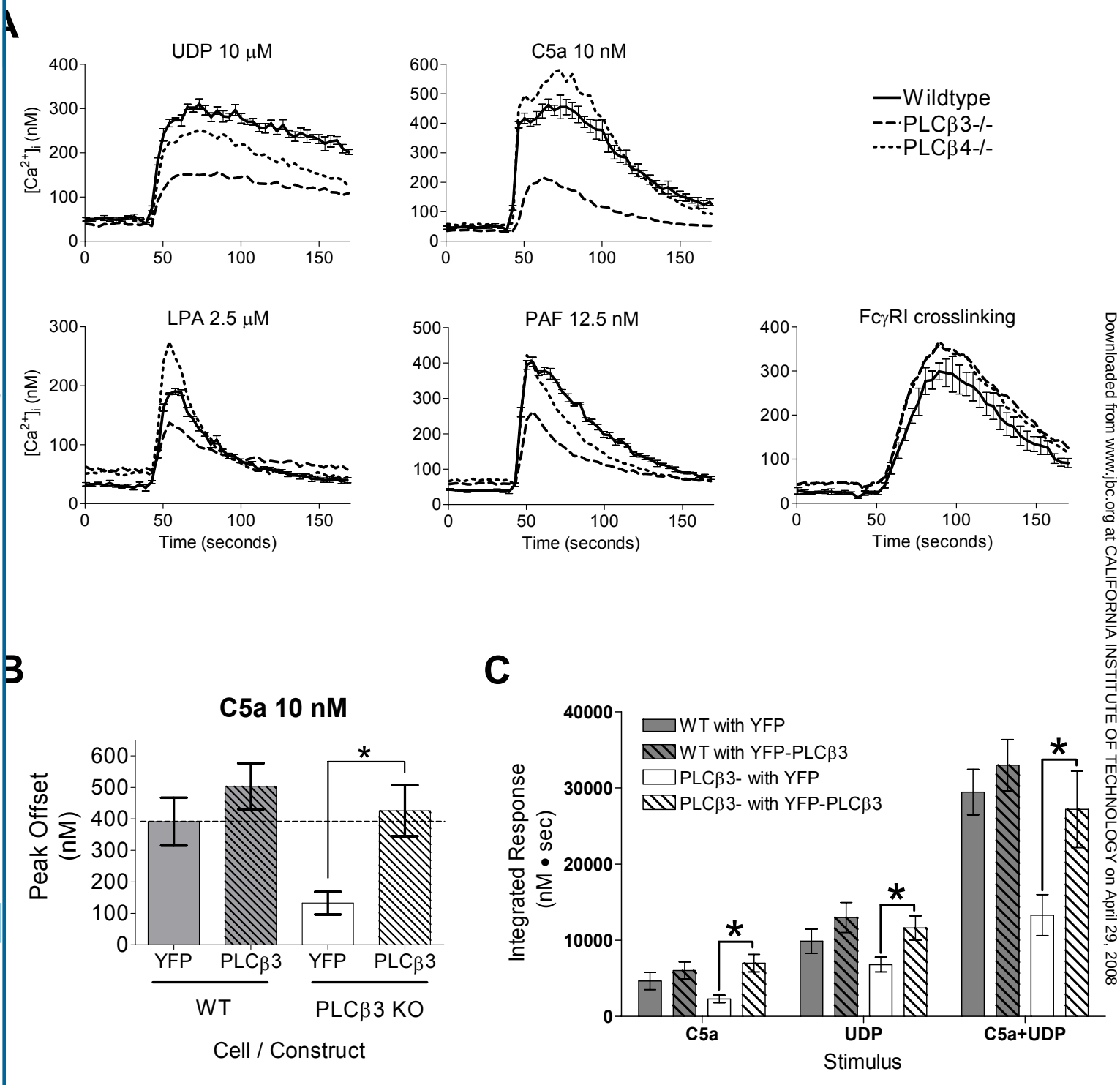

Figure 7

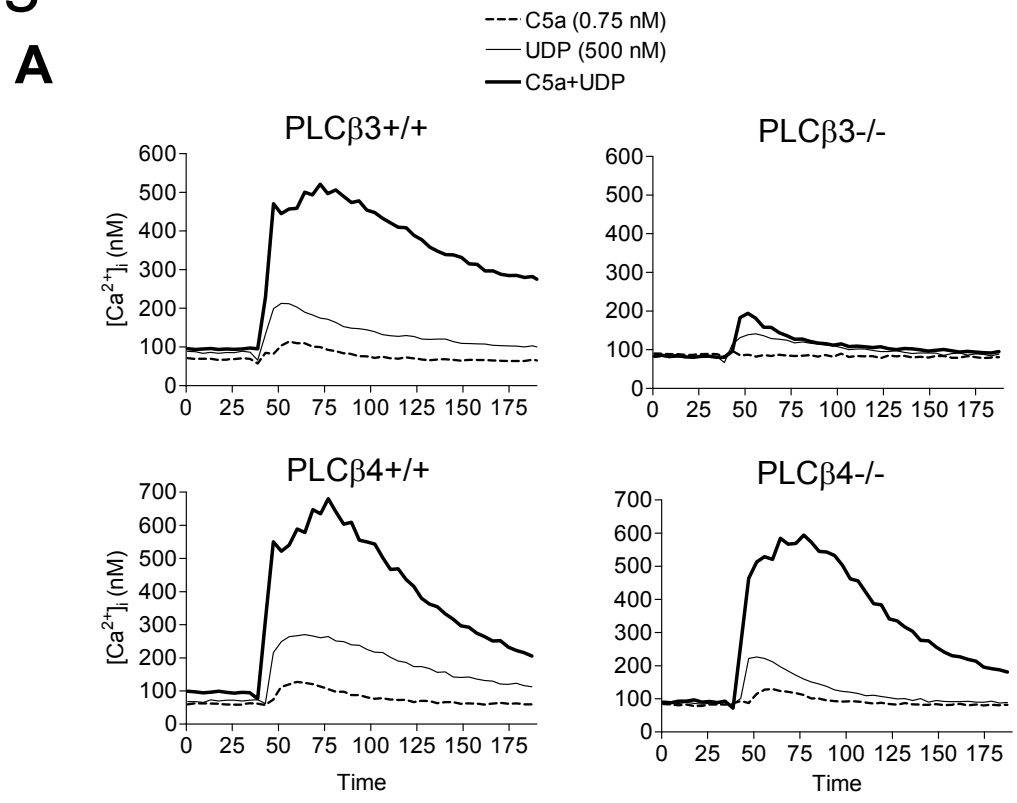

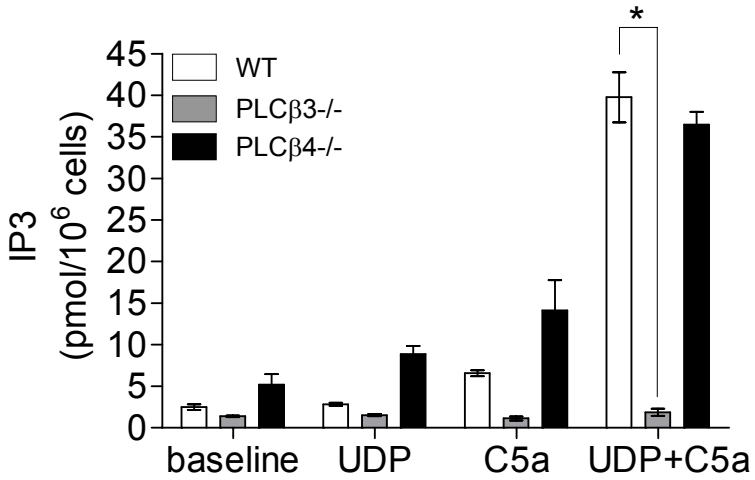

Figure 8

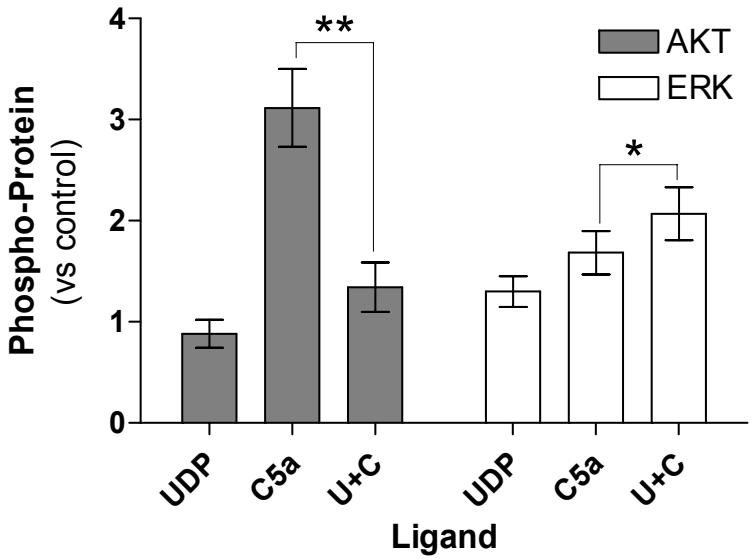

Figure 9